

Cover Page



Universiteit Leiden



The handle <http://hdl.handle.net/1887/20958> holds various files of this Leiden University dissertation.

**Author:** Sakalis, Philippe Alexandre

**Title:** Visualizing virulence proteins and their translocation into the host during agrobacterium-mediated transformation

**Issue Date:** 2013-06-12

# Chapter 2

---

## *In vivo* studies on the *Agrobacterium tumefaciens* virulence protein VirE2 reveal self-association at the microtubules

2



P. A. Sakalis, G.P.H. van Heusden and P.J.J. Hooykaas

Molecular and Developmental Genetics, Institute of Biology, Leiden University,  
Leiden, The Netherlands.

## ABSTRACT

**VirE2 is an effector protein involved in Agrobacterium-Mediated Transformation (AMT) of plant cells. Here we show, using both yeast cells and plant protoplasts, that a fluorescent VirE2 fusion protein is visible as a filament between the spindle poles in dividing cells and that these filamentous structures co-localize with microtubules. Bimolecular Fluorescence Complementation (BiFC) and Förster Resonance Energy Transfer (FRET) visualization studies show that VirE2 self-associates and physically interacts with the Tub1 tubulin. Moreover, using a BiFC assay, we showed that VirE2 interacts with the *Arabidopsis thaliana* VIP1 and Agrobacterium VirE3 proteins, both possibly involved in nuclear uptake of VirE2. These interactions co-localize with the spindle pole body component Spc42. Our data suggest a role for VirE2 in guiding the T-DNA complex to the host nucleus through transport along microtubule structures and a possible role of factors located at the spindle pole bodies in nuclear uptake of VirE2.**

## INTRODUCTION

*Agrobacterium tumefaciens* is a Gram negative soil-borne bacterium which causes tumor formation in dicotyledonous plant species by transferring oncogenic genes [1]. This unique trait makes the bacterium an interesting topic for biological studies. The genes that are transferred originate from the Transfer region (T-region) on a tumor-inducing plasmid (Ti plasmid) approximately 200 kbp in size [2]. Expression of the T-DNA genes in the plant cell leads to the synthesis of plant hormones causing uncontrolled cell proliferation and as a result tumor formation. These tumors are typically called crown galls. The transformed cells also produce opines, which can be specifically used by *A. tumefaciens* as a nitrogen source but not by most other organisms.

The T-DNA genes are translocated in a single stranded form (T-strand) via a type IV secretion system (T4SS) from the pathogen to the host organism. Apart from the T-strand also effector proteins are translocated via this T4SS. The genes encoding effector proteins (or virulence proteins) are located on the *vir* region of the Ti plasmid, together with the genes determining the T4SS. These effector proteins play a crucial role in the transformation process and are translocated to the plant cell independently from the T-strand [3].

The VirD2 protein is an essential effector protein for *Agrobacterium*-mediated transformation (AMT) of both plant and yeast cells. Inside *Agrobacterium* it is involved in generation of the T-strand. It contains a relaxase domain which is required to introduce site and strand specific nicks (single stranded breaks) in the border regions flanking the T-region [4][5]. Concomitantly with this event VirD2 becomes covalently attached to the 5' end of these nicks [6][7][8]. The released T-strand with VirD2 attached is subsequently translocated through the T4SS into the recipient cell, where it interacts with VirE2 virulence proteins to form a T-complex. In vitro assays have shown that VirE2 can bind ssDNA cooperatively irrespective of the sequence [9][10][11].

Inside the pathogen VirE2 is bound to its chaperone protein VirE1 [12] [13]. Recently the crystal structure of the VirE2-VirE1 complex has been resolved [14] which shows that VirE2 has a flexible linker separating two independent domains. This flexibility allows VirE2 to undergo structural rearrangements when bound to different binding partners. When unbound, VirE2 preferentially binds to other VirE2 proteins in an N- to C-terminal fashion forming long filamentous threads. The VirE1 protein, which is not translocated to the host, prevents this aggregation and also inhibits the ssDNA binding ability of VirE2 [15] inside the bacterium. Inside the host, the ssDNA binding property enables VirE2 to bind to the T-strand preventing host nuclease attacks of the translocated DNA molecule. The VirE2 protein contains two putative nuclear localization sequences (NLS) which, together with the C-terminal NLS of VirD2, aid nuclear uptake of the T-complex [16]. Possibly the interaction between VirE2 and the T-strand reshapes the complex in such a way that favors nuclear uptake of the complex [16]. In a yeast-two-hybrid screen for VirE2 binding partners, a plant host factor called VIP1 (VirE2 interacting protein 1) was identified [17]. In plants, VIP1 facilitates VirE2 nuclear intake and tumorigenicity [17]. It has been shown that VirE2 also interacts with the *Agrobacterium* virulence protein VirE3 [18]. The latter protein is translocated to the plant cell and it has been suggested that VirE3 can mimic the function of VIP1 by facilitating nuclear import of VirE2 [18]. In vitro studies have shown movement of “animalized” VirE2 across microtubules in a cell-free *Xenopus* egg extract [19], suggesting the nucleoprotein complex may travel to the nucleus with the help of cytoskeletal elements in the host rather than by simple diffusion.

Under laboratory circumstances - besides plants - many different organisms including yeast can be genetically transformed by *Agrobacterium* [20] [21][22]. This observation makes yeast a relevant model host organism to study and gain more insight in the mechanisms of AMT by using all the beneficial genetic tools that are readily available for the yeast *S. cerevisiae*. It has become the more

important as AMT has come to be the method of choice for the transformation of fungi.

VirE2 is not essential for the transformation of the yeast *S. cerevisiae* [20] and the filamentous fungus *Aspergillus awamori* [23]. Nevertheless, *A. tumefaciens*  $\Delta$ VirE2 mutants showed a tenfold lower frequency of T-DNA transfer to yeast and a more than two-fold lower transformation frequency of *A. awamori*. It has been shown that VirE2 is also translocated into yeast cells via the T4SS [24]. However, the localization and trafficking of ViE2 proteins in both the plant and yeast host cell is only partly understood. In this chapter we study the subcellular localization and dynamics of VirE2 inside the host using the yeast *Saccharomyces cerevisiae* as model host organism. Also the interactions of VirE2 with various binding partners were visualized in vivo to further our understanding of the biological processes underlying AMT. For this purpose we made use of the Bimolecular Fluorescence Complementation (BiFC) and Förster Resonance Energy Transfer (FRET) techniques. Our studies show that VirE2 filaments co-localize with microtubules in yeast, supporting the theory that VirE2 facilitates transport of the nucleoprotein complex along elements of the cytoskeleton. Secondly we show that VirE2 interacts with VIP1 and VirE3 at the spindle pole bodies, suggesting a role of these organelles in nuclear import of VirE2.

## MATERIALS AND METHODS

**Strains and Media.** Yeast strains used are listed in Table 1. Yeast was grown in YPD or MY supplemented if required with histidine, leucine, tryptophan and/ or uracil at final concentrations of 20 mg/L [25]. All yeast transformations were performed using the LiAc method [26]. Yeast strains carrying plasmids were obtained by transformation of the parental strains with the appropriate plasmids followed by selection for histidine and / or uracil prototrophy.

To study VirE2 in plant protoplasts we used *Arabidopsis thaliana* ecotype Col-0 protoplasts and performed protoplast transformations [27].

**Plasmid constructions.** All plasmids used and constructed in this study are listed in Table 2. Cloning steps were performed in *E. coli* strain DH5 $\alpha$ . PCR amplifications were done with *Phusion*<sup>TM</sup> *High-Fidelity* DNA Polymerase and Table 3 lists all primers used for PCR amplifications. The coding DNA sequences of *A. tumefaciens virE1*, *virE2* and *virE3* were PCR amplified from the pSDM3659 plasmid. A *Bam*HI-VirE1-*Eco*RI PCR fragment, amplified with *Bam*HI-VirE1-Fw and *Eco*RI-VirE1-Rev, was cloned into pJET1.2 generating pJET1.2[VirE1]. Subsequently a *Bam*HI-*Eco*RI fragment with VirE1 was cloned into vector pUG36YFP to generate pUG36YFP[VirE1]. In pUG36YFP[VirE1] VirE1 is N-terminally fused to YFP and transcription of the fusion protein is controlled by the *MET25* promoter and *CYC1* terminator. In order to clone VirE1 into pUG35, a PCR fragment with *Bam*HI-VirE1 $\Delta$ TGA-*Eco*RI, amplified using *Bam*HI-VirE1-Fw and *Eco*RI-VirE1 $\Delta$ TGA-Rev, was cloned into pJET1.2 generating pJET1.2[VirE1 $\Delta$ TGA]. Then, a *Bam*HI-*Eco*RI fragment with VirE1 $\Delta$ TGA was cloned into pUG35 to produce pUG35[VirE1]. pUG35[VirE1] has a C-terminal fusion of VirE1 to GFP and transcription is regulated by the *MET25* promoter and *CYC1* terminator.

A PCR fragment *Spe*I-VirE2-*Xma*I, amplified with *Spe*I-VirE2-Fw and *Xma*I-VirE2-Rev, was cloned into pJET1.2 generating pJET1.2[VirE2]. Subsequently, a *Spe*I-*Xma*I fragment with VirE2 was cloned into pUG34CFP and pUG36YFP to construct pUG34CFP[VirE2] and pUG36YFP[VirE2], respectively. PCR fragment *Spe*I-VirE2 $\Delta$ TGA-*Xma*I, amplified with *Spe*I-VirE2-Fw and *Xma*I-VirE2 $\Delta$ TGA-Rev, was cloned into pJET1.2 generating pJET1.2[VirE2 $\Delta$ TGA]. The *Spe*I-*Xma*I fragment with VirE2 $\Delta$ TGA was then cloned into pUG35 to make pUG35[VirE2]. VirE2 is N-terminally fused to CFP in pUG34CFP[VirE2] and to YFP in pUG36YFP[VirE2]. pUG35[VirE2] has a C-terminal fusion of VirE2 to GFP. Transcription of all VirE2 fusion proteins

in plasmids in pUG34CFP[VirE2], pUG36YFP[VirE2] and pUG35[VirE2] is regulated by the *MET25* promoter and *CYCI* terminator.

PCR fragment *SpeI*-VirE3-*EcoRI*, amplified with *SpeI*-VirE3-Fw and *EcoRI*-VirE3-Rev, was cloned into pJET1.2 generating pJET1.2[VirE3]. Next, a *SpeI*-*EcoRI* fragment with VirE3 was cloned into pUG36YFP to construct and pUG36YFP[VirE3].

For construction of BiFC plasmids we used the yeast tagging vectors EF210802 (pFA6a-VN-HIS3MX6) and EF210803 (pFA6a-VC-HIS3MX6) [28] as templates to PCR amplify the N- (VN) and C-terminal (VC) part of the coding DNA sequence from Venus [29]. BiFC plasmids pUG34VN, pUG34VC, pUG36VN and pUG36VC were constructed through replacement of a *XbaI*-*SpeI* fragment with CFP (in case of pUG34CFP) or YFP (in case of pUG36 YFP) by *XbaI*-*SpeI* fragments with VC or VN. These plasmids were used to generate N-terminal fusions with VN or VC under control of the *MET25* promoter and *CYCI* terminator. *XbaI*-VN-*SpeI* was obtained by PCR using *XbaI*-F2-Fw and *SpeI*-VN-Rev, subsequently cloned into pJET1.2 making pJET1.2[VNn], finally the *XbaI*-VN-*SpeI* fragment was ligated into *XbaI* and *SpeI* digested pUG34CFP and pUG36, generating pUG34VN and pUG36VN respectively. Similarly VC was amplified with *XbaI*-F2-Fw and *SpeI*-VC-Rev, cloned into pJET1.2 making pJET1.2[VCn] and the *XbaI*-VC-*SpeI* fragment was cloned into *XbaI* and *SpeI* digested pUG34 and pUG36, generating pUG34VC and pUG36VC respectively.

BiFC plasmids pUG35VN and pUG35VC were constructed to make C-terminal fusions with the BiFC parts VN and VC. Both VN and VC were amplified using *EcoRI*-F2-Fw and *EagI*-TADH1-Rev and cloned into pJET1.2 making pJET1.2[VNc] and pJET1.2[VCC], respectively. Subsequently the *EcoRI*-VN-TADH1-*EagI* fragments were cloned into *EcoRI* and *EagI* digested pUG35, replacing GFP by VN or VC and generating pUG35VN and pUG35VC. In these plasmids the original *CYCI* terminator is replaced by the *ADH1* terminator.

To make pUG36VN[VirE1] and pUG36VC[VirE1], a *BamHI*-VirE1-*EcoRI* fragment from pJET1.2[VirE1] was cloned into *BamHI* and *EcoRI* digested pUG36VN and pUG36VC, respectively. pUG35VN[VirE1] and pUG35VC[VirE1] were created by ligation of a *SpeI*-VirE1-*EcoRI* fragment from pUG35[VirE1] into *SpeI* and *EcoRI* digested pUG35VN and pUG35VC vectors.

pUG34VN[VirE2] and pUG36VN[VirE2] were constructed by cloning an *XbaI*-VN-*SpeI* fragment from pJET1.2[VNn] into *XbaI* and *SpeI* digested pUG34CFP[VirE2] and pUG36YFP[VirE2], respectively. pUG34VC[VirE2] and pUG36VC[VirE2] were constructed by cloning an *XbaI*-VC-*SpeI* fragment from

pJET1.2[VCn] into *XbaI* and *SpeI* digested pUG34[VirE2] and pUG36[VirE2], respectively. pUG35VN[VirE2] and pUG35VC[VirE2] were made by ligation of a *SpeI*-VirE2-*XmaI* fragment from pJET1.2[VirE2] into *SpeI* and *XmaI* digested pUG35VN and pUG35VC, respectively.

A *SpeI*-VirE3-*EcoRI* fragment from pJET1.2[VirE3] was cloned into *SpeI* and *EcoRI* digested pUG34VN and pUG34VC to create plasmids pUG34VN[VirE3] and pUG34VC[VirE3], respectively.

The coding DNA sequence of VirE2-interacting protein 1 (VIP1) was PCR amplified from plasmid pSDM3268 using *BamHI*-ViP1-Fw and *Sall*-ViP1-Rev and cloned into pCR-Blunt II-TOPO to make pTOPO[VIP1]. A *BamHI*-*Sall* fragment with VIP1 from pTOPO[VIP1] was then cloned into *BamHI* and *Sall* digested pUG34VN and pUG34VC to construct pUG34VN[VIP1] and pUG34VC[VIP1], respectively.

For studies on VirE2 movement we created the two plasmids pUG34PA-GFP[VirE2] and pUG34PGAL1[VirE2]. To amplify a 714 bp PA-GFP (photoactivatable GFP) without stop codon from template pYM48 [30] we used oligonucleotides *XbaI*-PA-GFP-Fw and *SpeI*-PA-GFP $\Delta$ TAA-Rev and cloned the obtained PCR product into pJET1.2 to construct pJET1.2[PA-GFP]. Subsequently a *XbaI*-PA-GFP $\Delta$ TAA-*SpeI* fragment was cloned into *XbaI* and *SpeI* digested pUG34CFP[VirE2], creating pUG34PA-GFP[VirE2]. The *GALI* promoter sequence was obtained by digestion of pYM-N25 [30] with *SacI* and *XbaI*, releasing a *SacI*-*XbaI* fragment with PGAL1. This fragment was ligated into *XbaI* and *SacI* digested pUG34CFP[VirE2], replacing the *MET25* promoter by PGAL1, to generate pUG34PGAL1[CFP-VirE2].

In order to study VirE2 localization in *A. thaliana* Col-0 protoplasts we cloned the VirE2 coding sequence into the pART7 based vector pART7-YFP [31]. A *SpeI* fragment with VirE2 from pSDM3163GFP11[VirE2] (P.A. Sakalis, unpublished) was cloned into *XbaI* digested pART7-YFP (C.S. Galvan Ampudia, unpublished) to make the pART7YFP[VirE2] vector.

For FRET analysis additional plasmids pRS306-Turquoise-TUB1, pUG34Turquoise, pUG34Turquoise[VirE2] and pUG34YFP were constructed. To make FRET plasmids containing the coding sequence of mTurquoise we used plasmid pmTurquoise-C1 [32] as template for PCR amplifications. PCR fragment *XhoI*-Turquoise-*BamHI*, amplified with *XhoI*-mTurquoise-Fw and *BamHI*-*SpeI*-Turquoise-Rev, was cloned into pJET1.2 generating pJET1.2[mTurquoise]. Plasmid pRS306-Turquoise-TUB1 was constructed by replacing the CFP encoding

*XhoI*-*Bam*HI fragment in pRS306-CFP-TUB1 [33] with a *XhoI*-*Bam*HI fragment containing mTurquoise from pJET1.2[mTurquoise]. A second PCR fragment *XbaI*-Turquoise-*SpeI*, amplified with *XbaI*-Turquoise-Fw and *Bam*HI-*SpeI*-Turquoise-Rev, was cloned into pJET1.2 generating pJET1.2[mTurquoise]-2. The mTurquoise encoding *XbaI*-*SpeI* fragment from this plasmid was ligated into *XbaI*-*SpeI* digested pUG34CFP and pUG34CFP[VirE2] to generate pUG34Turquoise and pUG34Turquoise[VirE2], respectively. Finally, plasmid pUG34YFP[VirE2] was constructed by replacing the CFP encoding *XbaI*-*SpeI* fragment in pUG34CFP with the YFP encoding *XbaI*-*SpeI* fragment from pUG36YFP.

All PCR fragments were verified by sequencing before using them for plasmid constructions. Correct ligation was checked by restriction analysis and sequencing.

**Microtubule disruptions.** Yeast strain MAS101-34CFP-VirE2 was grown overnight in MY medium with appropriate nutrients. The overnight culture was supplemented with benomyl at final concentration of 100  $\mu$ g/ml. Benomyl treatment was applied for 60 minutes and microscopic analysis on the benomyl treated yeast culture was performed with 10 minutes intervals, from 5 minutes until 60 minutes after addition of benomyl.

For disruption of microtubules in protoplasts we treated *A. thaliana* Col-0 protoplasts – transformed with pART7YFP[VirE2] – with oryzalin at a final concentration of 50  $\mu$ M. Microscopic analysis of oryzalin treated protoplasts was performed with 10 minutes intervals, from 20 minutes until 80 minutes after addition of oryzalin.

**Flow cytometry.** Parental strain CEN.PK113-3B (negative control for background fluorescence), BiFC control strains 428-34VC/35VN[VirE2] and 428-34VC[VirE2]/35VN, and 428-34VC[VirE2]/35VN[VirE2] were analyzed by flow cytometry. Yeast cells were grown in MY medium supplemented with the appropriate nutrients and diluted ten-fold before flow cytometry. The Guave EasyCyte™ system from MILLIPORE was used and data were analyzed with CytoSoft™ software. A 488 nm laser and a 510-540 nm band pass filter were used to detect YFP fluorescence. For each analysis 3000 cells were used.

**Confocal Microscopy.** Yeast cells were grown in MY medium supplemented with the appropriate nutrients. All microscopic analyses were done with confocal laser scanning microscopy (CLSM) using a Zeiss LSM 5 Exciter (Zeiss, Oberkochen,

Germany) using a 63x magnifying objective (numerical aperture 1.4). CFP signal was detected using an argon 458 nm laser and a 475-515 nm band pass filter. GFP signal was detected using an argon 488 nm laser and a 505-530 nm band pass filter. To detect YFP signal and reconstituted BiFC signal an argon 514 nm laser and a 530-600 nm band pass filter were used. Microscopic images were analyzed using ImageJ software [34] and assembled using Adobe Photoshop CS4 and Adobe Illustrator CS4.

**Förster Resonance Energy Transfer (FRET).** All yeast strains were grown overnight in MY medium supplemented with appropriate nutrients. Microscopy was performed as described above. FRET studies [35] on the interaction between VirE2 and Tub1p were done with a sensitized emission FRET approach. For this goal we used yeast strains 426-34Turquoise/36YFP (negative control) and 426::Turquoise-TUB1/34YFP-VirE2. Microscopic images were processed with ImageJ software, using the *FRET and Colocalization Analyzer* plugin [36] to measure sensitized emission FRET. Bleed through (BT) values were calculated with the plugin using images of yeast 426-34Turquoise-VirE2 (donor BT control) and 426-36YFP-VirE2 (acceptor BT control).

To study VirE2-VirE2 interactions the acceptor photobleaching FRET approach was used. Yeast strains 426-34Turquoise/36YFP, 426-34Turquoise-VirE2, 426-36YFP-VirE2 were used as negative controls and yeast strain 426-34Turquoise-VirE2/36YFP-VirE2 to measure FRET efficiency between VirE2 proteins. To photobleach the acceptor it was irradiated using an argon 514 nm laser for 5 minutes. Immediately after photobleaching (to prohibit fluorescence recovery of the acceptor) images were made to calculate FRET. The microscopic images were processed with ImageJ software, using the AccPbFRET plugin [37] to measure acceptor photobleaching FRET. Yeast strain 426-34Turquoise-VirE2 was used to calculate the correction factor  $\gamma$  for unwanted photobleaching of the donor. The correction factor  $\delta$ , for bleed through of acceptor in donor channel, was calculated using yeast strain 426-36YFP-VirE2. Finally,  $\epsilon$  corrects for an acceptor photoproduct which can contribute to the post-bleach donor signal. To calculate  $\epsilon$  we used yeast strain 426-36YFP-VirE2.

**Table 1: Yeast strains used in this study**

Yeast strain	Genotype	Source / reference
CEN.PK113-3B	<i>MA Talfa ura3-52 his3-delta1</i>	P. Kötter, Göttingen, Germany.
CEN.PK2-1C	<i>MATa ura3-52 leu2-112 trp1-289 his3-delta1</i>	P. Kötter, Göttingen, Germany.
MAS101 (AFS403)	<i>S. cerevisiae</i> pRS306[P <sub>HIS3</sub> -GFP-TUB1] ( <i>URA3</i> )	A. W. Murray, Harvard, U.S. [38]
SHM284-1	<i>MATa ura3-52 leu2delta1::pSM976 trp1delta63 his3delta200 SPC42-RFP-KanMX6</i>	Elmar Schiebel, Heidelberg, Germany [39]
428-35-VirE1-GFP (GG3340)	CEN.PK113-3B pUG35[P <sub>MET25</sub> -VirE1-GFP-T <sub>CYC1</sub> ] ( <i>URA3</i> )	This study
428-36YFP-VirE1 (GG3341)	CEN.PK113-3B pUG36[P <sub>MET25</sub> -YFP-VirE1-T <sub>CYC1</sub> ] ( <i>URA3</i> )	This study
428-34CFP-VirE2 (GG3342)	CEN.PK113-3B pUG34[P <sub>MET25</sub> -CFP-VirE2-T <sub>CYC1</sub> ] ( <i>HIS3</i> )	This study
428-36YFP-VirE2 (GG3343)	CEN.PK113-3B pUG36[P <sub>MET25</sub> -YFP-VirE2-T <sub>CYC1</sub> ] ( <i>URA3</i> )	This study
428-35-VirE2-GFP (GG3344)	CEN.PK113-3B pUG35[P <sub>MET25</sub> -VirE2-GFP-T <sub>CYC1</sub> ] ( <i>URA3</i> )	This study
428-36YFP-VirE3 (GG3345)	CEN.PK113-3B pUG36[P <sub>MET25</sub> -YFP-VirE3-T <sub>CYC1</sub> ] ( <i>URA3</i> )	This study
428-34CFP-VirE2 / 36YFP-VirE1 (GG3346)	CEN.PK113-3B pUG34[P <sub>MET25</sub> -CFP-VirE2-T <sub>CYC1</sub> ] ( <i>HIS3</i> ) pUG36[P <sub>MET25</sub> -YFP-VirE1-T <sub>CYC1</sub> ] ( <i>URA3</i> )	This study
MAS101-34CFP-VirE2 (GG3347)	MAS101 pUG34[P <sub>MET25</sub> -CFP-VirE2-T <sub>CYC1</sub> ] ( <i>HIS3</i> )	This study
284-34CFP-VirE2 (GG3348)	SHM284-1 (Spc42p-RFP) pUG34[P <sub>MET25</sub> -CFP-VirE2-T <sub>CYC1</sub> ] ( <i>HIS3</i> )	This study
428-34VN[VirE2]/35VC (GG3349)	CEN.PK113-3B pUG34[P <sub>MET25</sub> -VN-VirE2-T <sub>CYC1</sub> ] ( <i>HIS3</i> ) pUG35[P <sub>MET25</sub> -VC-T <sub>ADH1</sub> ] ( <i>URA3</i> )	This study
428-34VN[VirE2]/36VC (GG3350)	CEN.PK113-3B pUG34[P <sub>MET25</sub> -VN-VirE2-T <sub>CYC1</sub> ] ( <i>HIS3</i> ) pUG36[P <sub>MET25</sub> -VC-T <sub>CYC1</sub> ] ( <i>URA3</i> )	This study
428-34VC[VirE2]/35VN (GG3351)	CEN.PK113-3B pUG34[P <sub>MET25</sub> -VC-VirE2-T <sub>CYC1</sub> ] ( <i>HIS3</i> ) pUG35[P <sub>MET25</sub> -VN-T <sub>ADH1</sub> ] ( <i>URA3</i> )	This study
428-34VC[VirE2]/36VN (GG3352)	CEN.PK113-3B pUG34[P <sub>MET25</sub> -VC-VirE2-T <sub>CYC1</sub> ] ( <i>HIS3</i> ) pUG36[P <sub>MET25</sub> -VN-T <sub>CYC1</sub> ] ( <i>URA3</i> )	This study
428-34VN[VirE2]/35VC[VirE2] (GG3353)	CEN.PK113-3B pUG34[P <sub>MET25</sub> -VN-VirE2-T <sub>CYC1</sub> ] ( <i>HIS3</i> ) pUG35[P <sub>MET25</sub> -VirE2-VC-T <sub>ADH1</sub> ] ( <i>URA3</i> )	This study
428-34VN[VirE2]/36VC[VirE2] (GG3354)	CEN.PK113-3B pUG34[P <sub>MET25</sub> -VN-VirE2-T <sub>CYC1</sub> ] ( <i>HIS3</i> ) pUG36[P <sub>MET25</sub> -VC-VirE2-T <sub>ADH1</sub> ] ( <i>URA3</i> )	This study
428-34VC[VirE2]/35VN[VirE2] (GG3355)	CEN.PK113-3B pUG34[P <sub>MET25</sub> -VC-VirE2-T <sub>CYC1</sub> ] ( <i>HIS3</i> ) pUG35[P <sub>MET25</sub> -VirE2-VN-T <sub>ADH1</sub> ] ( <i>URA3</i> )	This study
428-34VC[VirE2]/36VN[VirE2] (GG3356)	CEN.PK113-3B pUG34[P <sub>MET25</sub> -VC-VirE2-T <sub>CYC1</sub> ] ( <i>HIS3</i> ) pUG36[P <sub>MET25</sub> -VN-VirE2-T <sub>ADH1</sub> ] ( <i>URA3</i> )	This study
428-34VN[VirE2]/35VC[VirE1] (GG3357)	CEN.PK113-3B pUG34[P <sub>MET25</sub> -VN-VirE2-T <sub>CYC1</sub> ] ( <i>HIS3</i> ) pUG35[P <sub>MET25</sub> -VirE1-VC-T <sub>ADH1</sub> ] ( <i>URA3</i> )	This study

428-34VN[VirE2]/36VC[VirE1] (GG3358)	CEN.PK113-3B pUG34[P <sub>MET25</sub> -VN-VirE2-T <sub>CYC1</sub> ] ( <i>HIS3</i> ) pUG36[P <sub>MET25</sub> -VC-VirE1-T <sub>ADH1</sub> ] ( <i>URA3</i> )	This study
428-34VC[VirE2]/35VN[VirE1] (GG3359)	CEN.PK113-3B pUG34[P <sub>MET25</sub> -VC-VirE2-T <sub>CYC1</sub> ] ( <i>HIS3</i> ) pUG35[P <sub>MET25</sub> -VirE1-VN-T <sub>ADH1</sub> ] ( <i>URA3</i> )	This study
428-34VC[VirE2]/36VN[VirE1] (GG3360)	CEN.PK113-3B pUG34[P <sub>MET25</sub> -VC-VirE2-T <sub>CYC1</sub> ] ( <i>HIS3</i> ) pUG36[P <sub>MET25</sub> -VN-VirE1-T <sub>ADH1</sub> ] ( <i>URA3</i> )	This study
428-34VN[VirE3]/35VC[VirE2] (GG3361)	CEN.PK113-3B pUG34[P <sub>MET25</sub> -VN-VirE3-T <sub>CYC1</sub> ] ( <i>HIS3</i> ) pUG35[P <sub>MET25</sub> -VirE2-VC-T <sub>ADH1</sub> ] ( <i>URA3</i> )	This study
428-34VC[VirE3]/35VN[VirE2] (GG3362)	CEN.PK113-3B pUG34[P <sub>MET25</sub> -VC-VirE3-T <sub>CYC1</sub> ] ( <i>HIS3</i> ) pUG35[P <sub>MET25</sub> -VirE2-VN-T <sub>ADH1</sub> ] ( <i>URA3</i> )	This study
284-34VN[VirE3]/35VC[VirE2] (GG3363)	SHM284-1 (Spc42p-RFP) pUG34[P <sub>MET25</sub> -VN-VirE3-T <sub>CYC1</sub> ] ( <i>HIS3</i> ) pUG35[P <sub>MET25</sub> -VirE2-VC-T <sub>ADH1</sub> ] ( <i>URA3</i> )	This study
284-34VC[VirE3]/35VN[VirE2] (GG3364)	SHM284-1 (Spc42p-RFP) pUG34[P <sub>MET25</sub> -VC-VirE3-T <sub>CYC1</sub> ] ( <i>HIS3</i> ) pUG35[P <sub>MET25</sub> -VirE2-VN-T <sub>ADH1</sub> ] ( <i>URA3</i> )	This study
428-34VN[VirP1]/35VC[VirE2] (GG3365)	CEN.PK113-3B pUG34[P <sub>MET25</sub> -VN-VirP1-T <sub>CYC1</sub> ] ( <i>HIS3</i> ) pUG35[P <sub>MET25</sub> -VirE2-VC-T <sub>ADH1</sub> ] ( <i>URA3</i> )	This study
428-34VC[VirP1]/35VN[VirE2] (GG3366)	CEN.PK113-3B pUG34[P <sub>MET25</sub> -VC-VirP1-T <sub>CYC1</sub> ] ( <i>HIS3</i> ) pUG35[P <sub>MET25</sub> -VirE2-VN-T <sub>ADH1</sub> ] ( <i>URA3</i> )	This study
284-34VN[VirP1]/35VC[VirE2] (GG3367)	SHM284-1 (Spc42p-RFP) pUG34[P <sub>MET25</sub> -VN-VirP1-T <sub>CYC1</sub> ] ( <i>HIS3</i> ) pUG35[P <sub>MET25</sub> -VirE2-VC-T <sub>ADH1</sub> ] ( <i>URA3</i> )	This study
284-34VC[VirP1]/35VN[VirE2] (GG3368)	SHM284-1 (Spc42p-RFP) pUG34[P <sub>MET25</sub> -VC-VirP1-T <sub>CYC1</sub> ] ( <i>HIS3</i> ) pUG35[P <sub>MET25</sub> -VirE2-VN-T <sub>ADH1</sub> ] ( <i>URA3</i> )	This study
428-34PA-GFP[VirE2] (GG3369)	CEN.PK113-3B pUG34[P <sub>MET25</sub> -PA-GFP-VirE2-T <sub>CYC1</sub> ] ( <i>HIS3</i> )	This study
428-34PGAL1[VirE2] (GG3370)	CEN.PK113-3B pUG34[P <sub>GAL1</sub> -CFP-VirE2-T <sub>CYC1</sub> ] ( <i>HIS3</i> )	This study
426-34Turquoise/36YFP (GG3371)	CEN.PK2-1C pUG34[P <sub>MET25</sub> -Turquoise-T <sub>CYC1</sub> ] ( <i>HIS3</i> ) pUG36[P <sub>MET25</sub> -YFP-T <sub>CYC1</sub> ] ( <i>URA3</i> )	This study
426-34Turquoise-VirE2 (GG3372)	CEN.PK2-1C pUG34[P <sub>MET25</sub> -Turquoise-VirE2-T <sub>CYC1</sub> ] ( <i>HIS3</i> )	This study
426-36YFP-VirE2 (GG3373)	CEN.PK2-1C pUG36[P <sub>MET25</sub> -YFP-VirE2-T <sub>CYC1</sub> ] ( <i>URA3</i> )	This study
426::Turquoise-TUB1/34YFP-VirE2 (GG3374)	CEN.PK2-1C <i>ura3</i> ::pRS306[P <sub>HIS3</sub> -Turquoise-TUB1-T <sub>HIS3</sub> ] ( <i>URA3</i> ) pUG34YFP ( <i>HIS3</i> )	This study
426-34Turquoise-VirE2/36YFP-VirE2 (GG3375)	CEN.PK2-1C pUG34[P <sub>MET25</sub> -Turquoise-VirE2-T <sub>CYC1</sub> ] ( <i>HIS3</i> ) pUG36[P <sub>MET25</sub> -YFP-VirE2-T <sub>CYC1</sub> ] ( <i>URA3</i> )	This study

**Table 2: Plasmids used in this study**

<b>Name</b>	<b>Properties</b>	<b>Source / reference</b>
pSDM3659	pBBR6 with 4.266 kb <i>virE</i> operon	Amke den Dulk, unpublished
pSDM3268	pBBR6 with 1.026 kb coding sequences of VIP1	C. Michiels, unpublished
pUG34CFP (pRUL1001)	Centromeric plasmid to make N-terminal CFP fusions under control of the <i>MET25</i> promoter and <i>CYC1</i> terminator. <i>HIS3</i> marker.	M. Miedema and G.P.H. van Heusden, unpublished
pUG35	Centromeric plasmid to make C-terminal GFP fusions under control of the <i>MET25</i> promoter and <i>CYC1</i> terminator. <i>URA3</i> marker.	U. Güldener and J.H. Hegemann, unpublished
pUG36YFP (pRUL1004)	Centromeric plasmid to make N-terminal YFP fusions under control of the <i>MET25</i> promoter and <i>CYC1</i> terminator. <i>URA3</i> marker.	M. Miedema and G.P.H. van Heusden, unpublished
pJET1.2	CloneJET™ PCR Cloning pUC19 based vector for blunt cloning	Fermentas UAB
pJET1.2[VirE1] (pRUL1234)	pJET1.2 with <i>virE1</i> flanked by <i>Bam</i> HI and <i>Eco</i> RI restriction sites.	This study
pJET1.2[VirE1ΔTGA] (pRUL1235)	pJET1.2 with <i>virE1</i> without stop codon flanked by <i>Bam</i> HI and <i>Eco</i> RI restriction sites.	This study
pJET1.2[VirE2] (pRUL1236)	pJET1.2 with <i>virE2</i> flanked by <i>Spe</i> I and <i>Xma</i> I restriction sites.	This study
pJET1.2[VirE2ΔTGA] (pRUL1237)	pJET1.2 with <i>virE2</i> without stop codon flanked by <i>Spe</i> I and <i>Xma</i> I restriction sites.	This study
pJET1.2[VirE3] (pRUL1238)	pJET1.2 with <i>virE3</i> flanked by <i>Spe</i> I and <i>Eco</i> RI restriction sites.	This study
pUG34YFP[VirE2] (pRUL1239)	Centromeric plasmid with YFP-VirE2 under control of <i>MET25</i> promoter and <i>CYC1</i> terminator. <i>HIS3</i> marker.	This study
pUG35[VirE1] (pRUL1240)	Centromeric plasmid with VirE1-GFP under control of <i>MET25</i> promoter and <i>CYC1</i> terminator. <i>URA3</i> marker.	This study
pUG36YFP[VirE1] (pRUL1241)	Centromeric plasmid with YFP-VirE1 under control of <i>MET25</i> promoter and <i>CYC1</i> terminator. <i>URA3</i> marker.	This study
pUG34CFP[VirE2] (pRUL1242)	Centromeric plasmid with CFP-VirE2 under control of <i>MET25</i> promoter and <i>CYC1</i> terminator. <i>HIS3</i> marker.	This study
pUG35[VirE2] (pRUL1243)	Centromeric plasmid with VirE2-GFP under control of <i>MET25</i> promoter and <i>CYC1</i> terminator. <i>URA3</i> marker.	This study
pUG36YFP[VirE2] (pRUL1244)	Centromeric plasmid with YFP-VirE2 under control of <i>MET25</i> promoter and <i>CYC1</i> terminator. <i>URA3</i> marker.	This study
pUG36YFP[VirE3] (pRUL1245)	Centromeric plasmid with YFP-VirE3 under control of <i>MET25</i> promoter and <i>CYC1</i> terminator. <i>URA3</i> marker.	This study
pFA6a-VN-His3MX6 (EF210802)	Yeast tagging pFA6a based vector containing 560 bp N-terminal part of Venus (VN).	Sung and Huh [28]
pFA6a-VC-His3MX6 (EF210803)	Yeast tagging pFA6a based vector containing 300 bp C-terminal part of Venus (VC).	Sung and Huh [28]
pJET1.2[VNn] (pRUL1246)	pJET1.2 with the N-terminal Venus part (VN) flanked by <i>Xba</i> I and <i>Spe</i> I restriction sites. The VN part is designed for N-terminal fusions.	This study

pJET1.2[VCn] (pRUL1247)	pJET1.2 with the C-terminal Venus part (VC) flanked by <i>Xba</i> I and <i>Spe</i> I restriction sites. The VC part is designed for N-terminal fusions.	This study
pJET1.2[VNc] (pRUL1248)	pJET1.2 with VN-TADH1 flanked by <i>Eco</i> RI and <i>Eag</i> I restriction sites. The VN part is designed for C-terminal fusions.	This study
pJET1.2[VCc] (pRUL1249)	pJET1.2 with VC-TADH1 flanked by <i>Eco</i> RI and <i>Eag</i> I restriction sites. The VC part is designed for C-terminal fusions.	This study
pUG34VN (pRUL1177)	Centromeric plasmid to make N-terminal fusions with the N-terminal Venus part under control of the <i>MET25</i> promoter and <i>CYC1</i> terminator. <i>HIS3</i> marker.	This study
pUG34VC (pRUL1176)	Centromeric plasmid to make N-terminal fusions with the C-terminal Venus part under control of the <i>MET25</i> promoter and <i>CYC1</i> terminator. <i>HIS3</i> marker.	This study
pUG35VN (pRUL1181)	Centromeric plasmid to make C-terminal fusions with the N-terminal Venus part under control of the <i>MET25</i> promoter and <i>ADH1</i> terminator. <i>URA3</i> marker.	This study
pUG35VC (pRUL1180)	Centromeric plasmid to make C-terminal fusions with the N-terminal Venus part under control of the <i>MET25</i> promoter and <i>ADH1</i> terminator. <i>URA3</i> marker.	This study
pUG36VN (pRUL1250)	Centromeric plasmid to make N-terminal fusions with the N-terminal Venus part under control of the <i>MET25</i> promoter and <i>CYC1</i> terminator. <i>URA3</i> marker.	This study
pUG36VC (pRUL1251)	Centromeric plasmid to make N-terminal fusions with the C-terminal Venus part under control of the <i>MET25</i> promoter and <i>CYC1</i> terminator. <i>URA3</i> marker.	This study
pUG35VN[VirE1] (pRUL1252)	Centromeric plasmid with <i>VirE1</i> -VN under control of the <i>MET25</i> promoter and <i>ADH1</i> terminator. <i>URA3</i> marker.	This study
pUG35VC[VirE1] (pRUL1253)	Centromeric plasmid with <i>VirE1</i> -VC under control of the <i>MET25</i> promoter and <i>ADH1</i> terminator. <i>URA3</i> marker	This study
pUG36VN[VirE1] (pRUL1254)	Centromeric plasmid with VN- <i>virE1</i> under control of the <i>MET25</i> promoter and <i>CYC1</i> terminator. <i>URA3</i> marker.	This study
pUG36VC[VirE1] (pRUL1255)	Centromeric plasmid with VC- <i>virE1</i> under control of the <i>MET25</i> promoter and <i>CYC1</i> terminator. <i>URA3</i> marker.	This study
pUG34VN[VirE2] (pRUL1256)	Centromeric plasmid with VN- <i>virE2</i> under control of the <i>MET25</i> promoter and <i>CYC1</i> terminator. <i>HIS3</i> marker.	This study
pUG34VC[VirE2] (pRUL1257)	Centromeric plasmid with VC- <i>virE2</i> under control of the <i>MET25</i> promoter and <i>CYC1</i> terminator. <i>HIS3</i> marker.	This study
pUG35VN[VirE2] (pRUL1258)	Centromeric plasmid with <i>VirE2</i> -VN under control of the <i>MET25</i> promoter and <i>ADH1</i> terminator. <i>URA3</i> marker.	This study
pUG35VC[VirE2] (pRUL1259)	Centromeric plasmid with <i>VirE2</i> -VC under control of the <i>MET25</i> promoter and <i>ADH1</i> terminator. <i>URA3</i> marker	This study

pUG36VN[VirE2] (pRUL1260)	Centromeric plasmid with <i>VN-virE2</i> under control of the <i>MET25</i> promoter and <i>CYC1</i> terminator. <i>URA3</i> marker.	This study
pUG36VC[VirE2] (pRUL1261)	Centromeric plasmid with <i>VC-virE2</i> under control of the <i>MET25</i> promoter and <i>CYC1</i> terminator. <i>URA3</i> marker.	This study
pUG34VN[VirE3] (pRUL1262)	Centromeric plasmid with <i>VN-virE3</i> under control of the <i>MET25</i> promoter and <i>CYC1</i> terminator. <i>HIS3</i> marker.	This study
pUG34VC[VirE3] (pRUL1263)	Centromeric plasmid with <i>VC-virE3</i> under control of the <i>MET25</i> promoter and <i>CYC1</i> terminator. <i>HIS3</i> marker.	This study
pCR-Blunt II-TOPO	Vector for high-efficiency DNA cloning of blunt-end PCR products	InVitrogen
pTOPO[ViP1]	PCR Blunt II TOPO containing <i>ViP1</i> flanked by <i>Bam</i> HI and <i>Sal</i> I restriction sites.	X. Niu, unpublished
pUG34VN[ViP1] (pRUL1264)	Centromeric plasmid with <i>VN-ViP1</i> under control of the <i>MET25</i> promoter and <i>CYC1</i> terminator. <i>HIS3</i> marker.	This study
pUG34VC[ViP1] (pRUL1265)	Centromeric plasmid with <i>VC-ViP1</i> under control of the <i>MET25</i> promoter and <i>CYC1</i> terminator. <i>HIS3</i> marker.	This study
pYM48	Plasmid with PCR tagging cassette containing coding sequence of photoactivatable GFP (PA-GFP).	EUROSCARF [30]
pYM-N25	Plasmid with PCR tagging cassette containing DNA sequence of <i>GAL1</i> promoter.	EUROSCARF [30]
pJET1.2[PA-GFP] (pRUL1266)	pJET1.2 with photoactivatable GFP (PA-GFP) flanked by <i>Xba</i> I and <i>Spe</i> I restriction sites.	This study
pUG34PA-GFP[VirE2] (pRUL1267)	Centromeric plasmid with <i>PA-GFP-VirE2</i> under control of the <i>MET25</i> promoter and <i>CYC1</i> terminator. <i>HIS3</i> marker.	This study
pUG34PGAL1[VirE2] (pRUL1268)	Centromeric plasmid with <i>CFP-VirE2</i> under control of the <i>GAL1</i> promoter and <i>CYC1</i> terminator. <i>HIS3</i> marker.	This study
pSDM3163GFP11[VirE2] (pSDM3756)	pSDM3163 based vector with coding sequence of GFP11- <i>VirE2</i> under control of <i>VirE</i> promoter and terminator.	P.A. Sakalis, Chapter 3
pART7-YFP (pRUL1269)	pART7 based vector with <i>YFP</i> under control of the 35S promoter and the octopine synthase ( <i>OCS</i> ) terminator.	C.S. Galvan Ampudia, unpublished
pART7-YFP[VirE2] (pRUL1270)	pART7 based vector with <i>YFP-VirE2</i> under control of the 35S promoter and the octopine synthase ( <i>OCS</i> ) terminator.	This study
pmTurquoise-C1	Mammalian expression vector with <i>mTurquoise</i>	Goedhart <i>et al.</i> [32]
pRS306-CFP-TUB1	Yeast integrative vector with <i>CFP-TUB1</i> under control of the <i>HIS</i> promoter and terminator. <i>URA3</i> marker.	Jensen <i>et al.</i> [33]
pJET1.2[Turquoise] (pRUL1271)	pJET1.2 with <i>mTurquoise</i> flanked by <i>Xho</i> I and <i>Bam</i> HI restriction sites.	This study
pJET1.2[Turquoise]-2 (pRUL1272)	pJET1.2 with <i>mTurquoise</i> flanked by <i>Xba</i> I and <i>Spe</i> I restriction sites.	This study
pRS306-Turquoise-TUB1 (pRUL1273)	Yeast integrative vector with <i>Turquoise-TUB1</i> under control of the <i>HIS</i> promoter and terminator. <i>URA3</i> marker.	This study
pUG34Turquoise (pRUL1274)	Centromeric plasmid to make N-terminal Turquoise fusions under control of the <i>MET25</i> promoter and <i>CYC1</i> terminator. <i>HIS3</i> marker.	This study

pUG34Turquoise[VirE2] (pRUL1275)	Centromeric plasmid with Turquoise-VirE2 under control of <i>MET25</i> promoter and <i>CYC1</i> terminator. <i>HIS3</i> marker.	This study
-------------------------------------	---	------------

**Table 3: Primers used in this study.**

Primer name	Sequence (5' → 3')
<i>Bam</i> HI-VirE1 Fw	CGGGATCCATGGCCATCATCAAGCC <sup>a</sup>
<i>Eco</i> RI-VirE1 Rev	CGGAATTCTCACTCCTTCTGACCAG
<i>Eco</i> RI-VirE1ΔTGA Rev	CGGAATTCTCCTTCTGACCAGCAA
<i>Spe</i> I-VirE2 Fw	GGACTAGTATGGATCTTTCTGGCAA
<i>Xma</i> I-VirE2 Rev	CCCCCGGGTCAAAGCTGTTGACGC
<i>Xma</i> I-VirE2ΔTGA Rev	CCCCCGGGAAGCTGTTGACGCTTT
<i>Spe</i> I-VirE3 Fw	GGACTAGTATGGTGAGCACTAC
<i>Eco</i> RI-VirE3 Rev	CGGAATTCTTAGAAACCTCTGGA
<i>Eco</i> RI-VirE3ΔTAA Rev	CGGAATTCGAAACCTCTGGAGGT
<i>Bam</i> HI-ViP1 Fw	AAGGATCCATGGAAGGAGGAGGAAGAGGACC
<i>Sal</i> I-ViP1 Rev	AAGTCGACTCAGCCTCTCTTGGTAAAATCCA
<i>Xba</i> I-F2 Fw	GCTCTAGAGGTCGACGGATCCCCGGGTT
<i>Spe</i> I-VN Rev	GGACTAGTAGTACCACCAGAACCCTCGATGTTGTGGCGGATC
<i>Spe</i> I-VC Rev	GGACTAGTAGTACCACCAGAACCCTTGTACAGCTCGTCCATG
<i>Eco</i> RI-F2 Fw	CGGAATTCCGGTCGACGGATCCCCGGGTT
<i>Eag</i> I-T <sub>ADH1</sub> Rev	GGCGGCCGGGCAAGCTAAACAGATCTA
<i>Xba</i> I-PA-GFP Fw	GCTCTAGAATGAGCAAGGGCGAG
<i>Spe</i> I-PA-GFPΔTAA Rev	GGACTAGTCTTGTACAGCTCGTC
<i>Xho</i> I-Turquoise Fw	CCCTCGAGATGGTGAGCAAGGGCGAGGA
<i>Bam</i> HI- <i>Spe</i> I-Turquoise Rev	AAGGATCCACTAGTCTTGTACAGCTCGTCCATGCC
<i>Xba</i> I-Turquoise Fw	AATCTAGAATGGTGAGCAAGGGCGA

a, restriction sites are underlined.

## RESULTS

### VirE2 co-localizes with microtubules in yeast

2

During AMT the virulence protein VirE2 is translocated through the T4SS from *Agrobacterium* into the host cell. To study the fate of VirE2 in *S. cerevisiae* cells we expressed YFP-VirE2, CFP-VirE2 and VirE2-GFP fusion proteins in the *S. cerevisiae* strain CEN.pk113-3B under control of the *MET25* promoter and *CYC1* terminator. Microscopic studies showed that all VirE2 fusion proteins (N-terminal fusions as well as the C-terminal GFP fusion to VirE2) can be stably expressed in yeast and interestingly they aggregate as thread-like structures within the yeast cells. Figure 1 shows the subcellular localization of CFP-VirE2 and VirE2-GFP.

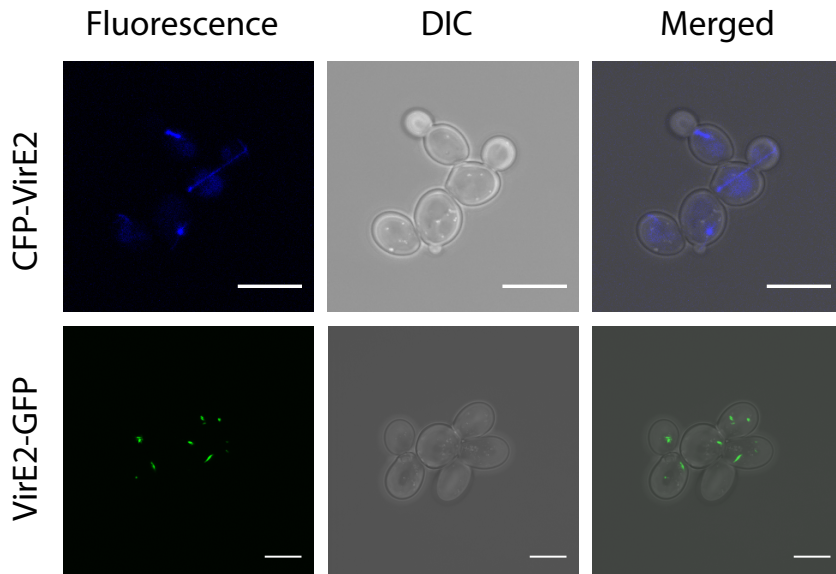


**Figure 1:** Subcellular localization of CFP-VirE2 in yeast strain 428-34CFP[VirE2] and VirE2-GFP in yeast strain 428-35[VirE2]. CFP-VirE2 and VirE2-GFP were expressed under control of the *MET25* promoter and *CYC1* terminator. Both CFP-VirE2 and VirE2-GFP fusion proteins aggregate as filamentous structures in yeast. Left: fluorescence (CFP in top image, GFP in bottom image); middle: visible field (DIC); right: fluorescence and visible images merged. Scale bars: 7  $\mu\text{m}$ .

The subcellular localization of VirE2 looked remarkably similar to that of microtubules. To investigate whether VirE2 indeed co-localizes with microtubules we expressed CFP-VirE2 in the yeast strain MAS101 which has a genomically integrated *GFP-TUB1* gene to visualize microtubules. Confocal

laser scanning microscopy (CLSM) showed that CFP-VirE2 indeed co-localized with GFP-Tub1p (Figure 2A).

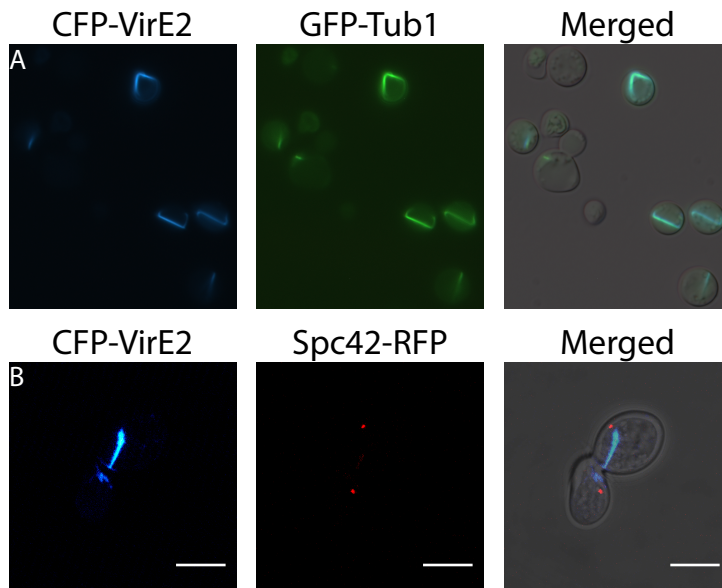


**Figure 2:** Confocal laser scanning microscopy of MAS101-34CFP-VirE2 (A) and 284-34CFP-VirE2 (B) cells shows that CFP-VirE2 filaments co-localize with microtubules (A) and that CFP-VirE2 filaments localize between the spindle poles of the mother and daughter cell in dividing cells (B). CFP-VirE2 was expressed under control of the *MET25* promoter and *CYC1* terminator in both yeast strains. (A) GFP-Tub1p was expressed under control of the *HIS3* promoter in strain MAS101-34CFP-VirE2. (B) Strain 284-34CFP-VirE2 expresses SPC42-RFP. Merged: fluorescence and visible images merged. Scale bars: 7  $\mu$ m.

Microtubules in dividing yeast cells are typically located between the two spindle poles [40]. To gain more evidence that VirE2 filaments in yeast localize in an identical manner as microtubules, we expressed CFP-VirE2 in strain SHM284-1 [39]. This strain expresses Spc42 C-terminally fused to RFP which localizes in the Spindle Pole Bodies. Microscopic analysis showed that CFP-VirE2 localizes in the same way as microtubules between the two spindle poles of the mother and daughter cell during cell division (Figure 2B).

To investigate whether disruption of microtubules influences the localization of CFP-VirE2, we exposed yeast cells expressing GFP-Tub1p and CFP-VirE2 to a relatively high dose of benomyl (100  $\mu$ g/ml). Benomyl is a microtubule-destabilizing drug [41][42] that inhibits polymerization of Tub1p subunits into microtubule structures in yeast [43]. Disruption of microtubule structures was observed approximately 45 minutes after the addition of benomyl

(Figure 3). At this time point both GFP-Tub1p and CFP-VirE2 filaments were broken. Fragments of the CFP-VirE2 filaments still co-localize with those of GFP-Tub1p filaments (Figure 3).

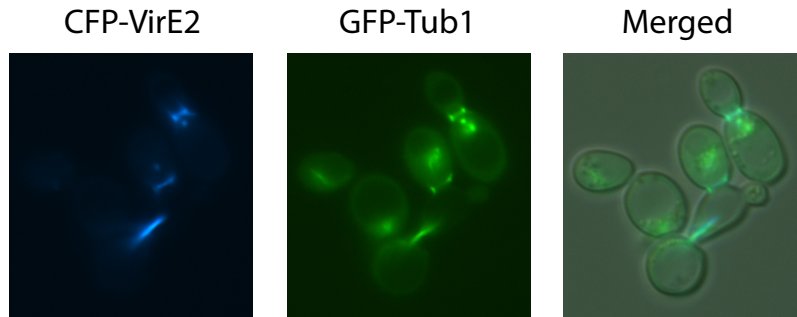


**Figure 3:** The microtubule-disturbing drug benomyl affects both the localization of CFP-VirE2 and GFP-Tub1p. MAS101-34CFP-VirE2 was exposed to 100  $\mu\text{g/ml}$  benomyl for 45 minutes and the localization of CFP-VirE2 and GFP-Tub1p was analyzed by confocal LSM microscopy. Left image: CFP fluorescence, middle image: GFP fluorescence, right image: CFP and GFP fluorescence merged with visible field.

### Visualization of VirE2 self-association

As shown in Figure 1, VirE2 is localized in filamentous structures. These structures may be formed by VirE2 self-association and/or by interaction of VirE2 with existing microtubule structures. Previous *in vitro* studies have shown that VirE2 can bind to other VirE2 molecules forming multi-protein structures [44]. In order to investigate whether VirE2 binds to itself in living yeast cells, we made use of the Bimolecular Fluorescence Complementation (BiFC) technique. This technique allows visualization of protein-protein interactions in the living cell and is based on the association of fluorescent protein fragments attached to sequences of two putative interaction-partner proteins. The fluorescence signal only appears if the studied proteins physically interact and the two fragments of the fluorescent protein, the YFP analog Venus in our case, come into close proximity to each other [28][45]. Confocal microscopy of cells expressing VirE2-VN (containing the N-terminal part of Venus, VN) and VC-VirE2 (containing the C-terminal part of Venus, VC) shows a clear fluorescent signal, indicating an interaction between VirE2 molecules (Figure 4A). The control cells with VirE2-VN and free VC or with free VN and VC-VirE2 have hardly detectable fluorescence. Similarly, control cells with VN-VirE2 and free VC or with VirE2-VC and free VN show next to no fluorescent signal (data not shown). This difference in fluorescence was also observed by using flow cytometry (Figure 4C), indicating a specific interaction

between VirE2-VN and VC-VirE2. We furthermore tested the combination VN-VirE2 with VC-VirE2 (Figure 4B) and VN-VirE2 with VirE2-VC (not shown). Although these interactions gave a detectable signal, the best signal was observed using cells expressing VC-VirE2 and VirE2-VN.

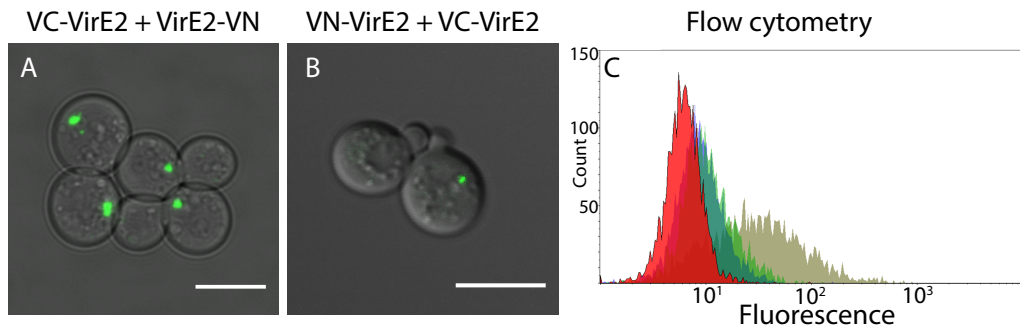


**Figure 4:** Visualization of interactions between VirE2 proteins by BiFC (A and B) and flow cytometry comparing VirE2 interactions with negative BiFC controls. Confocal LSM micrographs of (A) 428-34VC[VirE2]/35VN[VirE2] cells and (B) 428-34VN[VirE2]/36VC[VirE2] cells. (C) Flow cytometry histogram plot of CEN.PK113-3B (red), 428-34VC/35VN[VirE2] (blue), 428-34VC[VirE2]/35VN (green) and 428-34VC[VirE2]/35VN[VirE2] (olive). Scale bars: 7  $\mu$ m.

Another technique to visualize VirE2 – VirE2 interactions is the acceptor photobleaching Förster resonance energy transfer (FRET) technique. As reviewed by Swift and Trinkle-Mulcahy [46], this technique relies on the close physical interaction of two fluorophores, called donor and acceptor. The emission spectrum of the donor must overlap the excitation spectrum of the acceptor and the molecules must be within 10 nm of each other in order for FRET to occur. When two labeled proteins co-localize, the donor is quenched as the energy from the donor is transmitted to the acceptor. Acceptor photobleaching FRET relies on the principle that the donor fluorophore is de-quenched after photodestruction of the acceptor fluorophore. We used yeast strain 426::Turquoise-VirE2/36YFP-VirE2 expressing mTurquoise-VirE2 (donor) and YFP-VirE2 (acceptor) to study VirE2 – VirE2 binding. As shown in figure 5 A and B, both mTurquoise-VirE2 and YFP-VirE2 form filamentous structures. After photobleaching of YFP, the mTurquoise signal is somewhat increased (figure 5C). Using the AccPbFRET plugin for ImageJ [24] the FRET index was calculated and visualized in figure 5D. In a similar way, the negative control strain 426-34Turquoise/36YFP expressing unbound mTurquoise and unbound YFP was analyzed (figure 5E-H). The FRET index for the mTurquoise-VirE2 - YFP-VirE2 interaction is  $0.50 \pm 0.22$  (n=78) (mean  $\pm$  SD, for 78 positive pixels) compared to  $0.34 \pm 0.20$  (n=485) (mean  $\pm$  SD, for 485 positive pixels) for the mTurquoise – YFP interaction. Using the

Student's t-test, the former index is significantly higher than the latter one (two-tailed P value < 0.0001), in line with the interactions between VirE2 proteins observed with the BiFC technique. Images and calculations shown in Figure 5 are representative for other FRET experiments performed to study the interaction between VirE2 proteins.

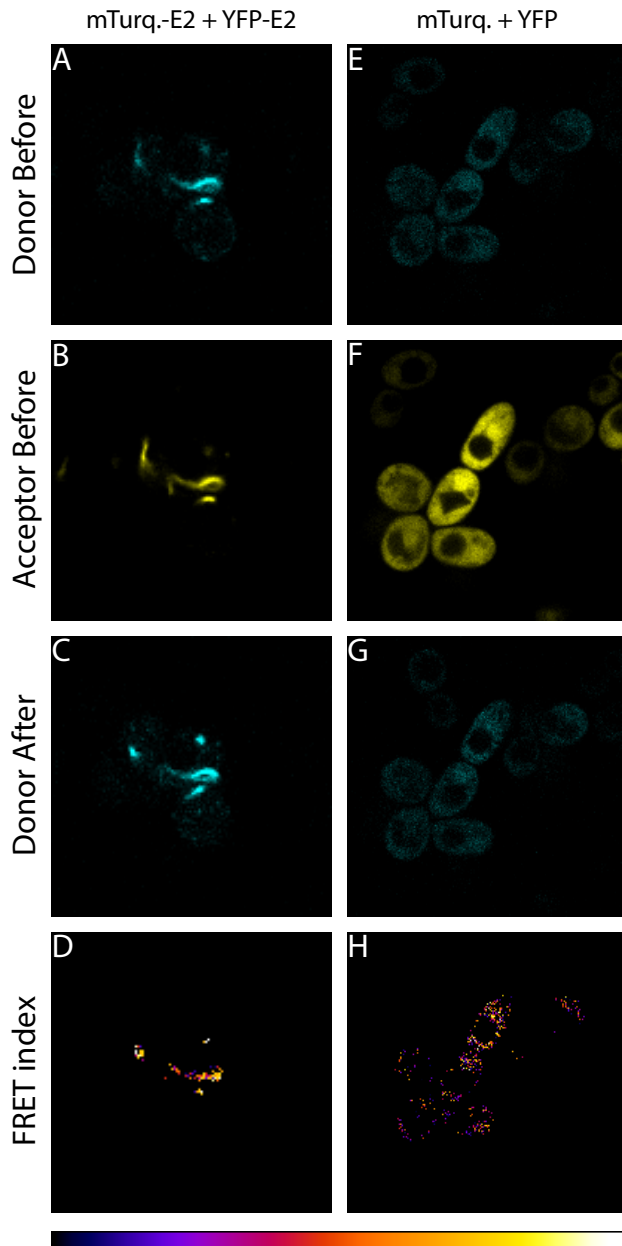


**Figure 5:**

Acceptor photobleaching FRET calculations using yeast strains 426::Turquoise-VirE2/36YFP-VirE2 and 426-34Turquoise/36YFP and ImageJ plugin AccPbFRET [37]. (A-D) Images and calculations using yeast strain 426::Turquoise-VirE2/36YFP-VirE2. Turquoise-VirE2 and YFP-VirE2 were expressed under control of the *MET25* promoter and *CYC1* terminator.

(E-H) Images and calculations using yeast strain 426-34Turquoise/36YFP as a negative control. Turquoise and YFP were expressed under control of the *MET25* promoter and *CYC1* terminator.

Before: Before photobleaching of the acceptor.

After: After 5 minutes photobleaching of the acceptor with 514 nm laser at 100 % intensity.

FRET index: FRET index images calculated by plugin AccPbFRET; look-up table: blue color indicating low values while yellow and white indicate high values.

## FRET experiments to analyze interactions of VirE2 with Tub1p

As shown in Figure 2, VirE2 filaments co-localize with tubulin filaments. Salman et al. have shown with *in vitro* experiments that VirE2 binds to microtubules [19]. To investigate whether this binding of VirE2 with tubulin could be visualized *in vivo* in yeast, we analyzed the interaction between mTurquoise-Tub1p and YFP-VirE2 by determining the energy transfer between the two fluorophores.

Adopting a sensitized emission approach to measure FRET, mTurquoise-Tub1p served as donor and YFP-VirE2 as acceptor. After excitation of the donor, fluorescence was measured in the acceptor channel only. In case of a physical interaction between the donor and the acceptor, some of the fluorescence measured in the acceptor channel is due to FRET. Using sensitized emission, measurements have to be corrected for donor bleed through and acceptor bleed through as they would lead to an overestimation of FRET. Fluorescence measured in the acceptor channel coming from the donor is termed donor bleed through. Alternatively, the acceptor may be directly excited by light used to excite the donor and this is called acceptor bleed through.

To measure FRET by sensitized emission, the ImageJ plugin *FRET and Colocalization Analyzer* [36] was used. This plugin allows calculation of a FRET index on a pixel by pixel basis and corrects for donor bleed through (DBT), acceptor bleed through (ABT) and false FRET (by associating FRET with co-localization of the two fluorophores). A “donor only” yeast strain expressing mTurquoise-VirE2 (426-34Turquoise-VirE2) and an “acceptor only” yeast strain expressing YFP-VirE2 (426-36YFP-VirE2) were used to determine DBT and ABT, respectively. Using these yeast strains we obtained a mean DBT value of 0.164 and a mean ABT value of 0.375. Microscopy of the strain expressing both mTurquoise-Tub1p and YFP-VirE2 showed co-localization of both proteins and a clear YFP signal was detectable after excitation of the mTurquoise (FRET signal) (Figure 6A). Correction for the DBT and ABT yielded a FRET index as visualized in Figure 6A. In a similar way the negative control strain expressing unbound mTurquoise and unbound YFP was analyzed and the FRET index calculated (Figure 6B).

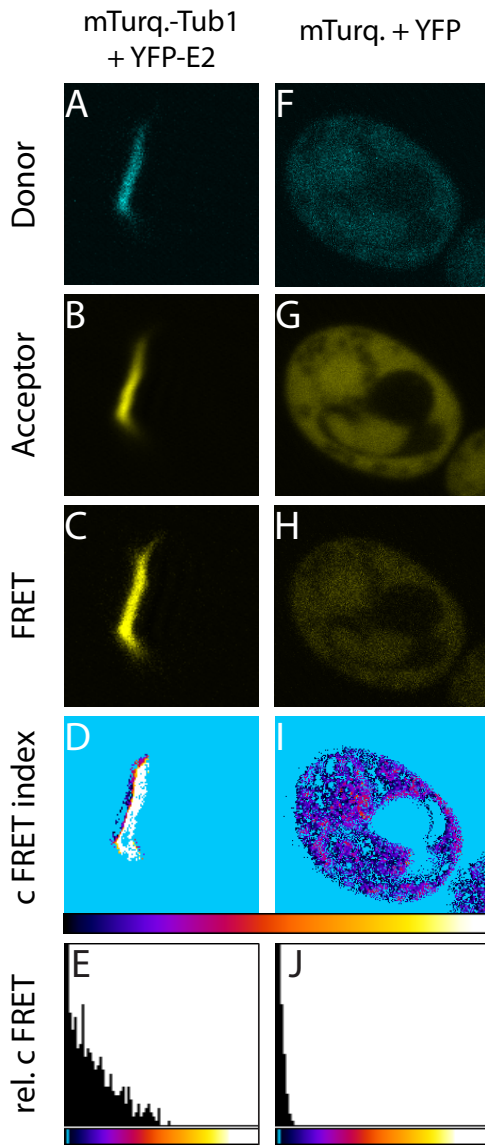


**Figure 6:** Analysis of FRET between mTurquoise-Tub1p and YFP-VirE2. Confocal LSM images of yeast strain 426::Turquoise-TUB1[YFP-VirE2] (A-E) and of the control strain 426-34Turquoise-36YFP (F-J) and the ImageJ plugin *FRET and Colocalization Analyzer* [36] were used to calculate the co-localized FRET (cFRET) index.

(A-E) FRET analysis on 426::Turquoise-TUB1[YFP-VirE2] expressing mTurquoise-Tub1 and YFP-VirE2. (A) mTurquoise-Tub1 as FRET donor imaged with CFP filter settings and (B) YFP-VirE2 as FRET acceptor imaged with YFP filter settings.

(F-J) FRET analysis on 426-34Turquoise-36YFP expressing free mTurquoise and free YFP. (F) Unbound mTurquoise as FRET donor imaged with the CFP filter settings and (G) unbound YFP as FRET acceptor imaged with the YFP filter settings.

(C and H) FRET image was taken with YFP emission filter after excitation at 458 nm (CFP excitation). (D and I) Calculation with the *FRET and Colocalization Analyzer* plugin rendered the cFRET index.

Relative cFRET indices were calculated for the mTurquoise-Tub1p – YFP-VirE2 pair (E) and for the unbound mTurquoise – unbound YFP pair (J) by dividing the calculated cFRET index by 20% of the pixel values from donor fluorescence images. Color bars represent minimal to maximal FRET intensities using “Fire” look-up-table from ImageJ.

The FRET index was corrected for the level of the donor fluorophore and, as seen in Figure 6E and 6J, the relative FRET index for mTurquoise-Tub1p - YFP-VirE2 pair was higher than that of the unbound mTurquoise – YFP pair. The relative FRET index for the mTurquoise-VirE2 - YFP-VirE2 interaction is  $11.9 \pm 9.0$  ( $n=384$ ) (mean  $\pm$  SD, for 384 positive pixels) compared to  $1.8 \pm 1.1$  ( $n=5801$ ) (mean  $\pm$  SD, for 5801 positive pixels) for the mTurquoise – YFP interaction. Using the Student’s t-test the former index is significantly ( $P<0.0001$ ) higher

that the latter one, suggesting that mTurquoise-Tub1p interacts with YFP-VirE2. Images and calculations shown in Figure 6 are representative for other FRET experiments performed to study the interaction between Tub1p and VirE2.

### Analysis of VirE2 movement along microtubules in yeast

Co-localization of VirE2 with microtubules is in support of the hypothesis that VirE2 moves along the microtubules in the direction of the nucleus thus contributing to the transfer of the T-complex into the nucleus. In line with this suggestion, Salman *et al.* [19] have shown that VirE2 is able to move along microtubules using a *Xenopus* cell free extract. To study movement of VirE2 in yeast we adopted two different strategies to visualize directional movement of VirE2 along microtubules. Firstly we induced CFP-VirE2 expression making use of the inducible *GALI* promoter and followed the CFP-VirE2 proteins over time. Secondly, we induced fluorescence of photoactivatable GFP (PA-GFP) [47][48] fused to VirE2 and followed fluorescently activated VirE2 over time.

Using the first strategy, yeast strain 428-34PGAL1[CFP-VirE2] was grown on galactose induction medium. Earliest CFP-VirE2 expression was observed approximately six hours after induction on galactose medium. This CFP-VirE2 signal was present in thread-like structures like those shown in Figure 1. After detection of the first signal, yeast cells were immediately transferred from galactose to glucose containing medium, inhibiting further CFP-VirE2 production, and the fluorescent signal was followed for approximately two hours with microscopy. However, no change in localization or movement of CFP-VirE2 could be detected.

Alternatively to protein induction, we induced fluorescence of PA-GFP-VirE2 in yeast strain 428-34PA-GFP[VirE2] by irradiation at 405 nm for 30 seconds. Subsequently, the activated PA-GFP-VirE2 signal was followed by microscopy over a time-period of two hours. Again, no movement of the activated PA-GFP-VirE2 was observed during these experiments.

### Analysis of the effect of single stranded DNA on the localization of VirE2 in yeast

Binding of effector protein VirE2 to the single stranded T-strand in the T-complex may reshape VirE2 in such a way that nuclear localization signals are exposed facilitating nuclear uptake. To study the effect of ssDNA on the localization of CFP-VirE2, we electroporated yeast strain MAS101-34CFP-VirE2 expressing GFP-Tub1p and CFP-VirE2 with single stranded salmon sperm

DNA. However, microscopy showed no obvious alterations in the localization of GFP-Tub1p and CFP-VirE2 at several time points, ranging from 15 minutes to 120 minutes after electroporation (data not shown).

### VirE2 localization in Arabidopsis protoplasts

2

In order to investigate the localization of VirE2 in plant cells, we transiently expressed YFP-VirE2 in *Arabidopsis* protoplasts. Thread-like structures of YFP-VirE2 were observed in the transformed protoplasts, comparable to those observed in yeast (see Chapter 4, Figure 1A and 1B). To visualize the effect of microtubule disruption on the VirE2 localization, protoplasts were treated with oryzalin, a herbicide that destabilizes microtubular structures by strongly binding to tubulin monomers [49]. Approximately one hour after the start of oryzalin treatment we saw a significant change in VirE2 localization, in line with our benomyl experiments in yeast. Thread-like YFP-VirE2 structures were either completely abolished (Chapter 4, Figure 1C) or severely shortened (Chapter 4, Figure 1D).

### Visualization of interactions of VirE2 with other proteins involved in AMT (VirE1, VIP1 and VirE3)

Inside *Agrobacterium* VirE1 binds to VirE2 thus preventing oligomerization of VirE2 prior to its transfer to the host cell [12][13][50]. To study interaction between VirE2 and VirE1 yeast strains expressing the BiFC pairs VN-VirE2 -- VirE1-VC, VN-VirE2 -- VC-VirE1, VC-VirE2 -- VirE1-VN and VC-VirE2 -- VN-VirE1 were analyzed. In all these strains we observed a relatively low fluorescence all over the yeast cell (data not shown). Confocal microscopy of control strains did not result in a detectable fluorescent signal, indicating a specific interaction between VirE1 and VirE2. We next expressed YFP-VirE1 together with CFP-VirE2 to investigate whether VirE1 disturbs VirE2 self-association. As shown in Figure 7, both CFP and YFP fluorescence were detected all over the yeast cell, indicating that VirE2 self-association was inhibited by expression of YFP-VirE1. Interestingly, in some yeast cells, with a lower YFP-VirE1 expression, VirE2 filament remnants were still visible (arrowhead in Figure 7).

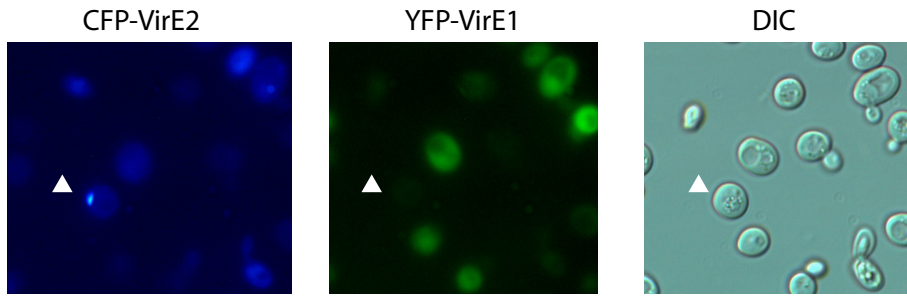


**Figure 7:** VirE1 inhibits VirE2 self-association. Confocal LSM images of yeast strain 428-34CFP-VirE2/36YFP-VirE1 expressing CFP-VirE2 and YFP-VirE1. CFP fluorescence is displayed blue, YFP fluorescence is displayed green. DIC: Differential interface contrast image. Arrowhead: CFP-VirE2 filament in yeast cell with relatively low YFP-VirE1 expression.

Using a BiFC approach, Lacroix *et al.* [18] showed VirE2 interactions with both VIP1 and VirE3 occurring mainly in the nucleus of plant cells (tobacco and onion). They also found indications that VirE3 facilitates nuclear import of VirE2 in mammalian (COS-1) cells. VIP1, is a plant bZIP transcription factor involved in the plant stress response [51], but *Agrobacterium* has captured this protein for nuclear import of the T-complex [17][52]. To assess the subcellular localizations of VIP1 and VirE3 in yeast we expressed CFP-VIP1 and YFP-VirE3 in yeast. We observed a nuclear localization for CFP-VIP1 (Figure 8A), whereas YFP-VirE3 localizes in dot shaped structures, possibly corresponding to the spindle pole bodies (Figure 8B). To analyze binding of VirE2 to VIP1 and VirE3 VC-VIP1 and VirE2-VN and VN-VirE2 and VC-VirE3, respectively, were co-expressed. Co-expression of VC-VIP1 and VirE2-VN resulted in a relatively strong fluorescence signal in dots near the nucleus (Figure 8C, green signal), while co-expression of VN-VirE2 and VC-VirE3 resulted in a strong fluorescence signal in dots (Fig. 8D, green signal). Co-expression of VC-VirE2 with VN-VIP1 and of VirE2-VC with VN-VirE3 resulted in negligible fluorescence. Thus, in contrast to the findings of Lacroix *et al.* [18] in plant cells, we did not observe a nuclear localization of VirE2 – VIP1 and VirE2 – VirE3 interactions. Instead, both interactions similarly localized as discrete dots inside the yeast cell. Studies with yeast strain SHM284-1 expressing Spc42-RFP which is localized at the spindle pole bodies, revealed that the VirE2 – VIP1 and VirE2 – VirE3 interactions co-localize with the spindle poles (Figure 8C and 8D).

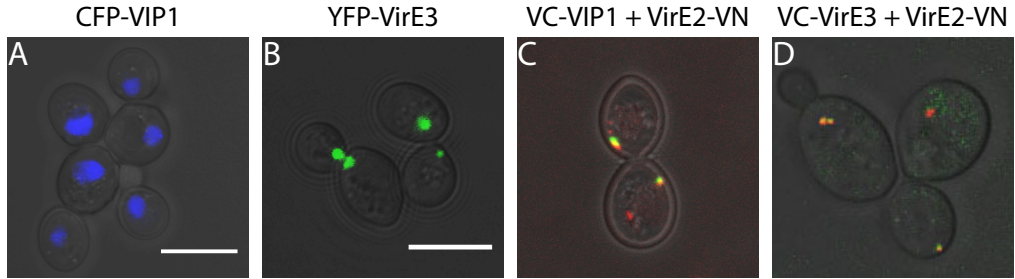


**Figure 8:** Subcellular localizations of CFP-ViP1, YFP-VirE3 and interactions of VirE2-ViP1 and VirE2-VirE3. Confocal LSM images of (A) yeast strain 426-34CFP-ViP1, CFP fluorescence, (B) yeast strain 428-36YFP-VirE3, YFP fluorescence, (C) yeast strain 284-34VC-ViP1/35VN-VirE2 and (D) yeast strain 284-34VC-VirE3/35VN-VirE2. Scale bar, 7 $\mu$ m. CFP-ViP1 in (A) shows nuclear localization and YFP-VirE3 in (B) localizes as dots inside the cell. Interactions VirE2 – ViP1 in (C) and VirE2 – VirE3 in (D) co-localize as discrete spots with the Spindle pole marker Spc42-RFP. YFP fluorescence resulting from BiFC is displayed green, RFP fluorescence is displayed red. The visible, YFP and RFP images were superimposed.

## DISCUSSION

During *Agrobacterium*-mediated transformation of both plants and the yeast *S. cerevisiae* the virulence protein VirE2 is transferred through the T4SS into the host cell. Here, the VirE2 protein binds to the T-strand in a cooperative way forming the T-complex [9][10]. In this way, the T-strand is protected against nucleolytic degradation, and the bipartite NLSs in VirE2 help in targeting the T-complex into the nucleus. As yet, many details of VirE2 functions in the host cells are still unknown. To further understand the behavior of VirE2 in the host cell we started in this study with the visualization of VirE2 and its interaction with other (virulence) proteins. For visualization studies yeast has several advantages above plants cells. First, yeast cells are transparent and do not contain large amounts of endogenous fluorescent compounds, like chlorophyll. Second, it is relatively easy to make strains stably expressing different combinations of tagged proteins. Previous studies from our [20][53] and other labs [21][54] have shown that yeast is an excellent organism to study AMT of eukaryotic cells.

A number of studies have been published to reveal the localization of VirE2 inside the host cell. As reviewed by Gelvin [55] the localization of VirE2 in the host cell is not unambiguous. Some studies find a cytoplasmic localization; other studies show nuclear import of VirE2. In this study we find a clear localization of VirE2 at the microtubules. This was observed after expression of both N- and C-terminally tagged VirE2, both in yeast (Figure 1) and in Arabidopsis protoplasts (Chapter 4, Figure 1). At the moment we have no explanation for the different localizations observed in our study compared to that found in some other studies. In support of a localization of VirE2 at the microtubules, VirE2 has been shown to bind to microtubules [19]. To further investigate a physical interaction between tubulin protein Tub1p and VirE2, FRET analysis was performed with Turquoise-Tub1p and YFP-VirE2. Turquoise is an enhanced form of CFP, recently developed by Goedhart *et al.* [32], which is beneficial for FRET studies compared to other CFP variants. These studies show that there is indeed energy transfer between the fluorophores. This energy transfer implies that the two fluorophores are in close proximity, indicative of a physical interaction between the two proteins. These observations are in line with the microtubular localization of VirE2 observed in our studies.

Krispin *et al.* [44] observed *in vitro* VirE2 oligomerization in the absence of VirE1 resulting in the formation of filamentous aggregates. Here we showed, using the BiFC technique, that *in vivo* VirE2 binds to other VirE2 molecules and that this binding is inhibited in the presence of VirE1. In our BiFC experiments, the strongest fluorescent signal was observed after expressing N-terminally

tagged VC-VirE2 together with C-terminally tagged VirE2-VN. This is in accordance with the crystal structure of the VirE1-VirE2 complex presented by Dym *et al.* [14], showing the tendency of VirE2 molecules to self-assemble in an N- to C-terminal manner. Acceptor photobleaching FRET studies on VirE2 – VirE2 interactions in yeast validated the results from this BiFC assay (Figure 5).

As mentioned before, Salman *et al.* [19] have shown that VirE2 is able to move along microtubules in *in vitro* experiments. In this study we were not able to detect movement of VirE2 proteins along the microtubules *in vivo* in yeast cells. To study movement of VirE2 in yeast we used two different strategies. Firstly, we induced CFP-VirE2 expression making use of the inducible *GALI* promoter and followed the CFP-VirE2 proteins over time. Secondly, we induced fluorescence of photoactivatable GFP (PA-GFP) [40][41] fused to VirE2 and followed fluorescently activated VirE2 over time. Possibly, expression of CFP-VirE2 under control of the *GALI* promoter resulted in high levels of the protein, resulting in complete colonization of microtubules which made it impossible to detect movement. Similarly, PA-GFP-VirE2 expression might have already led to complete VirE2 colonization of the microtubules. As a consequence no movement of a fluorescently activated sub-population of PA-GFP-VirE2 was detected. In another study, during cocultivation experiments, we have visualized translocation of VirE2 from *Agrobacterium* to yeast in real-time (Chapter 3). In those experiments a directional movement of VirE2 was indeed detected, in accordance with findings of Salman *et al.* [19].

Nuclear import of the T-complex is an important step in AMT of eukaryotic cells. VirE2 interacts with the plant bZIP transcription factor VIP1 [17] and upon phosphorylation of VIP1 by MPK3, VIP1 relocates from the cytoplasm to the nucleus [52]. In this way, nuclear import of the T-complex may be facilitated. Expression of CFP-VIP1 in yeast results in an exclusive nuclear localization (Figure 8). Apparently, phosphorylation may not be necessary for a nuclear localization in yeast or VIP1 may be constitutively phosphorylated by a yeast (MAP) kinase. Using BiFC we confirmed the interaction between VirE2 and VIP1 in yeast cells and interestingly this interaction co-localizes with the spindle pole body protein Spc42 (Figure 8C). VIP1 is a plant specific protein and yeast seems to lack an ortholog of VIP1. Possibly other yeast proteins have a similar function. Alternatively, the *Agrobacterium* virulence protein VirE3 fulfills this function in yeast. This virulence protein was shown to be translocated into the yeast cell during AMT [24]. Lacroix *et al.* [18] suggested that VirE3 has similar properties as the plant VIP1 protein. Upon expression in yeast YFP-VirE3

localizes in dot shaped structures, possibly corresponding to the spindle pole bodies (Figure 8B). The interaction of VirE3 with VirE2 was shown by BiFC to co-localize with the spindle pole body protein Spc42 (Figure 8D), similarly as the interaction between VirE2 and VIP1. Although the exact mechanism of nuclear import of VirE2 is still unknown, our results strongly suggest a role of the spindle pole bodies or components localized in close proximity to these organelles in the nuclear import of VirE2.

Concluding, the main findings discussed in this chapter are summarized in Figure 9: (1) VirE2 co-localizes with microtubules in yeast; (2) VirE2 self-associates; (3) VirE2 interacts with Tub1p; (4) the plant VIP1 has a nuclear localization in yeast; (5) VirE2 binds to VIP1 at the spindle pole bodies; (6) VirE3 localizes at the spindle pole bodies; (7) VirE2 binds to VirE3 at the spindle pole bodies; and (8) the above findings suggest a role of the microtubules and the spindle pole bodies in the nuclear uptake of the T-complex.

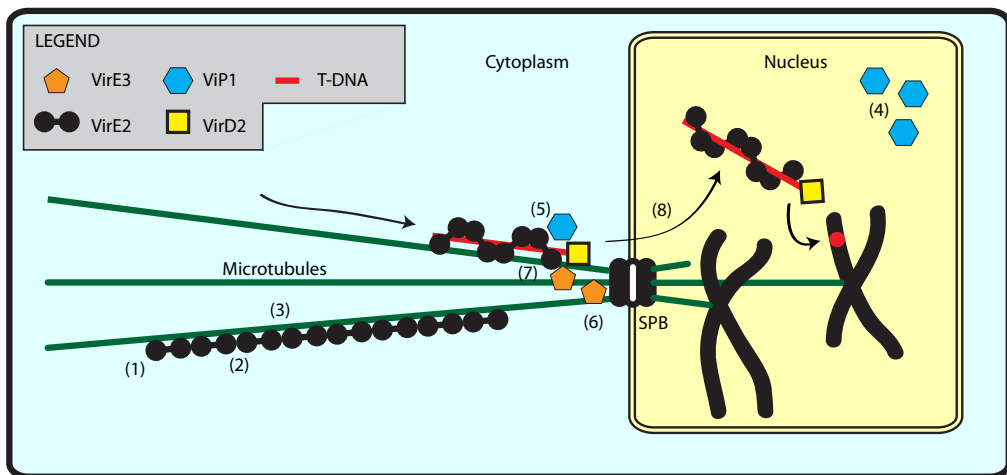


**Figure 9:** Simplified model of AMT of a host cell including the main findings discussed in this chapter (numbered 1 – 8). (1) VirE2 co-localizes as filaments with microtubules in yeast; (2) VirE2 binds to other VirE2 proteins; (3) VirE2 interacts with the microtubular subunit Tub1p; (4) the plant specific protein VIP1 has a nuclear localization in yeast; (5) VirE2 interacts with VIP1 at the spindle pole bodies; (6) VirE3 localizes at the spindle pole bodies; (7) VirE2 binds to VirE3 at the spindle pole bodies; (8) this model proposes a role of microtubules and the spindle pole bodies in nuclear uptake of the T-complex. SPB: spindle pole bodies. Arrows indicate directional movement of the T-complex during AMT.

## ACKNOWLEDGEMENTS

We thank Theodorus Gadella (Swammerdam Institute for Life Sciences, University of Amsterdam) for plasmid pmTurquoise-C1, Won-Ki Huh (School of Biological Sciences, Seoul National University) for the BiFC plasmids, Aryandi Kertokalio for help with setting up the BiFC experiments, Amke den Dulk-Ras for the *A. tumefaciens* deletion strains, Xiaolei Niu for images of yeast 426-34CFP-ViP1 and plasmid pTOPO[ViP1], Jessica Spadon for help with FRET studies and Gerda Lamers for the invaluable technical assistance with microscopy. This research has been funded by the division Chemical Sciences (CW) of the Netherlands Organization of Research (NWO), TOP-grant number 700.56.303.

## REFERENCES

1. Cleene DDL: **The host range of crown gall.** *Bot. Rev.* 1976, **42**:389–466.
2. Schrammeijer B, Beijersbergen A, Idler KB, Melchers LS, Thompson D V, Hooykaas PJ: **Sequence analysis of the vir-region from *Agrobacterium tumefaciens* octopine Ti plasmid pTi15955.** *J. Exp. Bot.* 2000, **51**:1167–9.
3. Vergunst AC, Schrammeijer B, Den Dulk-Ras A, De Vlaam CM, Regensburg-Tuink TJ, Hooykaas PJJ: **VirB/D4-dependent protein translocation from *Agrobacterium* into plant cells.** *Science* 2000, **290**:979–982.
4. Yanofsky MF, Porter SG, Young C, Albright LM, Gordon MP, Nester EW: **The *virD* operon of *Agrobacterium tumefaciens* encodes a site-specific endonuclease.** *Cell* 1986, **47**:471–477.
5. Jayaswal RK, Veluthambi K, Gelvin SB, Slightom JL: **Double-stranded cleavage of T-DNA and generation of single-stranded T-DNA molecules in *Escherichia coli* by a *virD*-encoded border-specific endonuclease from *Agrobacterium tumefaciens*.** *J. Bacteriol.* 1987, **169**:5035–45.
6. Young C, Nester EW: **Association of the VirD2 protein with the 5' end of T strands in *Agrobacterium tumefaciens*.** *J. Bacteriol.* 1988, **170**:3367–74.
7. Dürrenberger F, Crameri A, Hohn B, Koukolíková-Nicola Z: **Covalently bound VirD2 protein of *Agrobacterium tumefaciens* protects the T-DNA from exonucleolytic degradation.** *Proc. Natl. Acad. Sci. U.S.A.* 1989, **86**:9154–8.
8. Pansegrau W, Schoumacher F, Hohn B, Lanka E: **Site-specific cleavage and joining of single-stranded DNA by VirD2 protein of *Agrobacterium tumefaciens* Ti plasmids: analogy to bacterial conjugation.** *Proc. Natl. Acad. Sci. U.S.A.* 1993, **90**:11538–42.
9. Citovsky V, Wong ML, Zambryski P: **Cooperative interaction of *Agrobacterium* VirE2 protein with single-stranded DNA: implications for the T-DNA transfer process.** *Proc. Natl. Acad. Sci. U.S.A.* 1989, **86**:1193–7.
10. Sen P, Pazour GJ, Anderson D, Das A: **Cooperative binding of *Agrobacterium tumefaciens* VirE2 protein to single-stranded DNA.** *J. Bacteriol.* 1989, **171**:2573–2580.
11. Grange W, Duckely M, Husale S, Jacob S, Engel A, Hegner M: **VirE2: a unique ssDNA-compacting molecular machine.** *PLoS Biol.* 2008, **6**:343–351.
12. Sundberg C, Meek L, Carroll K, Das A, Ream W: **VirE1 protein mediates export of the single-stranded DNA-binding protein VirE2 from *Agrobacterium tumefaciens* into plant cells.** *J. Bacteriol.* 1996, **178**:1207–12.
13. Deng W, Chen L, Peng WT, Liang X, Sekiguchi S, Gordon MP, Comai L, Nester EW: **VirE1 is a specific molecular chaperone for the exported single-stranded-DNA-binding protein VirE2 in *Agrobacterium*.** *Mol. Microbiol.* 1999, **31**:1795–807.

14. Dym O, Albeck S, Unger T, Jacobovitch J, Branzburg A, Michael Y, Frenkiel-Krispin D, Wolf SG, Elbaum M: **Crystal structure of the *Agrobacterium* virulence complex VirE1-VirE2 reveals a flexible protein that can accommodate different partners.** *Proc. Natl. Acad. Sci. U.S.A.* 2008, **105**:11170–5.
15. Sundberg CD, Ream W: **The *Agrobacterium tumefaciens* chaperone-like protein, VirE1, interacts with VirE2 at domains required for single-stranded DNA binding and cooperative interaction.** *J. Bacteriol.* 1999, **181**:6850–5.
16. Ziemienowicz a, Merkle T, Schoumacher F, Hohn B, Rossi L: **Import of *Agrobacterium* T-DNA into plant nuclei: two distinct functions of VirD2 and VirE2 proteins.** *Plant Cell* 2001, **13**:369–83.
17. Tzfira T, Vaidya M, Citovsky V: **VIP1, an *Arabidopsis* protein that interacts with *Agrobacterium* VirE2, is involved in VirE2 nuclear import and *Agrobacterium* infectivity.** *EMBO J.* 2001, **20**:3596–607.
18. Lacroix B, Vaidya M, Tzfira T, Citovsky V: **The VirE3 protein of *Agrobacterium* mimics a host cell function required for plant genetic transformation.** *EMBO J.* 2005, **24**:428–37.
19. Salman H, Abu-Arish A, Oliel S, Loyter A, Klafater J, Granek R, Elbaum M: **Nuclear localization signal peptides induce molecular delivery along microtubules.** *Biophys. J.* 2005, **89**:2134–45.
20. Bundock P, Den Dulk-Ras A, Beijersbergen A, Hooykaas PJ: **Trans-kingdom T-DNA transfer from *Agrobacterium tumefaciens* to *Saccharomyces cerevisiae*.** *EMBO J.* 1995, **14**:3206–14.
21. Roberts RL, Metz M, Monks DE, Mullaney ML, Hall T, Nester EW: **Purine synthesis and increased *Agrobacterium tumefaciens* transformation of yeast and plants.** *Proc. Natl. Acad. Sci. U.S.A.* 2003, **100**:6634–9.
22. Bundock P, Mróczek K, Winkler AA, Steensma HY, Hooykaas PJ: **T-DNA from *Agrobacterium tumefaciens* as an efficient tool for gene targeting in *Kluyveromyces lactis*.** *Molecular general genetics MGG* 1999, **261**:115–121.
23. Michielse CB, Ram AFJ, Hooykaas PJJ, Hondel CAMJJ Van Den: ***Agrobacterium*-Mediated Transformation of *Aspergillus awamori* in the absence of full-length VirD2 , VirC2 , or VirE2 Leads to insertion of aberrant T-DNA structures.** *J. Bacteriol.* 2004, **186**:2038–2045.
24. Schrammeijer B: **Analysis of Vir protein translocation from *Agrobacterium tumefaciens* using *Saccharomyces cerevisiae* as a model: evidence for transport of a novel effector protein VirE3.** *Nucleic Acids Research* 2003, **31**:860–868.
25. Zonneveld BJM: **Cheap and simple yeast media.** *Journal of Microbiological Methods* 1986, **4**:287–291.
26. Gietz RD, Schiestl RH, Willems AR, Woods RA: **Studies on the transformation of intact yeast cells by the LiAc/SS-DNA/PEG procedure.** *Yeast* 1995, **11**:355–360.

27. Schirawski J, Planchais S, Haenni AL: **An improved protocol for the preparation of protoplasts from an established *Arabidopsis thaliana* cell suspension culture and infection with RNA of turnip yellow mosaic tymovirus: a simple and reliable method.** *Journal of Virological Methods* 2000, **86**:85–94.
28. Sung M, Huh W: **Bimolecular fluorescence complementation analysis system for in vivo detection of protein – protein interaction in *Saccharomyces cerevisiae*.** *Yeast* 2007, **24**:767–775.
29. Nagai T, Iбата K, Park ES, Kubota M, Mikoshiba K, Miyawaki A: **A variant of yellow fluorescent protein with fast and efficient maturation for cell-biological applications.** *Nature Biotechnology* 2002, **20**:87–90.
30. Janke C, Magiera MM, Rathfelder N, Taxis C, Reber S, Maekawa H, Moreno-Borchart A, Doenges G, Schwob E, Schiebel E, Knop M: **A versatile toolbox for PCR-based tagging of yeast genes: new fluorescent proteins, more markers and promoter substitution cassettes.** *Yeast* 2004, **21**:947–62.
31. Gleave AP: **A versatile binary vector system with a T-DNA organisational structure conducive to efficient integration of cloned DNA into the plant genome.** *Plant Molecular Biology* 1992, **20**:1203–1207.
32. Goedhart J, Van Weeren L, Hink MA, Vischer NOE, Jalink K, Gadella TWJ: **Bright cyan fluorescent protein variants identified by fluorescence lifetime screening.** *Nature Methods* 2010, **7**:137–139.
33. Jensen S, Segal M, Clarke DJ, Reed SI: **A novel role of the budding yeast separin Esp1 in anaphase spindle elongation: evidence that proper spindle association of Esp1 is regulated by Pds1.** *The Journal of Cell Biology* 2001, **152**:27–40.
34. Abràmoff MD, Hospitals I, Magalhães PJ, Abràmoff M: **Image Processing with ImageJ.** *Biophotonics Int* 2004, **11**:36–42.
35. Forster T: **Zwischenmolekulare Energiewanderung und Fluoreszenz.** *Ann Phys* 1948, **437**:55–75.
36. Hachet-Haas M, Converset N, Marchal O, Matthes H, Gioria S, Galzi J-L, Lecat S: **FRET and colocalization analyzer--a method to validate measurements of sensitized emission FRET acquired by confocal microscopy and available as an ImageJ Plug-in.** *Microscopy Research and Technique* 2006, **69**:941–956.
37. Roszik J, Szöllosi J, Vereb G: **AccPbFRET: an ImageJ plugin for semi-automatic, fully corrected analysis of acceptor photobleaching FRET images.** *BMC Bioinformatics* 2008, **9**:346.
38. Straight a. F: **Mitosis in living budding yeast: anaphase A but no metaphase plate.** *Science (80- )* 1997, **277**:574–578.

39. Pereira G, Tanaka TU, Nasmyth K, Schiebel E: **Modes of spindle pole body inheritance and segregation of the Bfa1p-Bub2p checkpoint protein complex.** *EMBO J.* 2001, **20**:6359–70.
40. Moens PB, Rapport E: **Spindles, spindle plaques, and meiosis in the yeast *Saccharomyces cerevisiae* (Hansen).** *The Journal of Cell Biology* 1971, **50**:344–61.
41. Thomas JH, Neff NF, Botstein D: **Isolation and characterization of mutants in the  $\beta$ -tubulin gene of *Saccharomyces cerevisiae*.** *Genetics* 1985, **112**:715–734.
42. Schatz PJ, Solomon F, Botstein D: **Isolation and characterization of conditional-lethal mutations in the *TUB1 a*-tubulin gene of the yeast *Saccharomyces cerevisiae*.** *Genetics* 1988, **120**:681–695.
43. Jacobs CW, Adams AEM, Szaniszló PJ, John R: **Functions of microtubules in the *Saccharomyces cerevisiae* cell cycle.** *J. Cell Biol.* 1988, **107**:1409–1426.
44. Frenkiel-Krispin D, Wolf SG, Albeck S, Unger T, Peleg Y, Jacobovitch J, Michael Y, Daube S, Sharon M, Robinson C V, Svergun DI, Fass D, Tzfira T, Elbaum M: **Plant transformation by *Agrobacterium tumefaciens*: modulation of single-stranded DNA-VirE2 complex assembly by VirE1.** *J. Biol. Chem.* 2007, **282**:3458–64.
45. Hu C-D, Chinenov Y, Kerppola TK: **Visualization of interactions among bZIP and Rel family proteins in living cells using bimolecular fluorescence complementation.** *Mol. Cell* 2002, **9**:789–98.
46. Swift SR, Trinkle-Mulcahy L: **Basic principles of FRAP, FLIM and FRET.** *Proceedings of the Royal Microscopical Society* 2004, **39**:3–10.
47. Patterson GH, Lippincott-Schwartz J: **A photoactivatable GFP for selective photolabeling of proteins and cells.** *Science (80- )* 2002, **297**:1873–7.
48. Patterson GH, Lippincott-Schwartz J: **Selective photolabeling of proteins using photoactivatable GFP.** *Methods* 2004, **32**:445–50.
49. Baskin TI, Wilson JE, Cork A, Williamson RE: **Morphology and microtubule organization in *Arabidopsis* roots exposed to oryzalin or taxol.** *Plant cell physiology* 1994, **35**:935–942.
50. Zhao Z, Sagulenko E, Ding Z, Christie PJ: **Activities of *virE1* and the VirE1 secretion chaperone in export of the multifunctional VirE2 effector via an *Agrobacterium* Type IV secretion pathway.** *J. Bacteriol.* 2001, **183**:3855–3865.
51. Pitzschke A, Djamei A, Teige M, Hirt H: **VIP1 response elements mediate mitogen-activated protein kinase 3-induced stress gene expression.** *Proc. Natl. Acad. Sci. U.S.A.* 2009, **106**:18414–9.
52. Djamei A, Pitzschke A, Nakagami H, Rajh I, Hirt H: **Trojan horse strategy in *Agrobacterium* transformation: abusing MAPK defense signaling.** *Science (80- )* 2007, **318**:453–456.

53. Van Attikum H, Bundock P, Hooykaas PJ: **Non-homologous end-joining proteins are required for *Agrobacterium* T-DNA integration.** *EMBO J.* 2001, **20**:6550–8.
54. Kiyokawa K, Yamamoto S, Sato Y, Momota N, Tanaka K, Moriguchi K, Suzuki K: **Yeast transformation mediated by *Agrobacterium* strains harboring an Ri plasmid: comparative study between *GALLS* of an Ri plasmid and *virE* of a Ti plasmid.** *Genes Cells* 2012, **17**:597–610.
55. Gelvin SB: **Finding a way to the nucleus.** *Curr. Opin. Microbiol.* 2010, **13**:53–8.

